



## From Biowaste to Biomaterials: Buffalo Teeth Derived Hydroxyapatite Based Biocomposites for Bone Tissue Applications

K. MANIVANNAN<sup>1</sup>, G. JAGANATHAN<sup>1</sup> and M. ABOOBUCKER SITHIQUE<sup>2\*</sup>

PG and Research Department of Chemistry, Islamiah College (Autonomous), Vaniyambadi-635751, India

\*Corresponding author: E-mail: [masithique2@gmail.com](mailto:masithique2@gmail.com)

Received: 26 April 2021;

Accepted: 4 October 2021;

Published online: 20 April 2022;

AJC-20755

The present study reported the preparation of food industry biowaste buffalo teeth-derived hydroxyapatite (BT-HA)/chitosan-polyvinyl pyrrolidone (CS-PVP)/aloe vera (ALV) natural biopolymer as a biocomposite for improved mechanical, antimicrobial and cytocompatible characteristics. The strengthening of biopolymer has a major role to play in improving the mechanical properties of the biocomposite, while the addition of aloe vera increases antimicrobial and cytocompatibility. Chemical structure, crystalline phase, morphology and mechanical property biocomposite were studied by FTIR, XRD, SEM-EDX and micro-hardness tests, respectively. Additionally, the antimicrobial effectiveness of the biocomposites was evaluated using Gram-positive and Gram-negative bacteria. The cytocompatibility of osteoblast cells to the biocomposites was calculated by the MTT assay examination. The findings demonstrated that the prepared biocomposite has the necessary mechanical, antimicrobial and biocompatible characteristics. Generally, the mixture of mechanical characteristics of CS-PVP, the antimicrobial and cytocompatible property of aloe vera in BT-HA/CS-PVP/ALV, makes the biocomposite a prospective restorative substance for various clinical applications.

**Keywords:** Hydroxyapatite, Biocomposite, Bone, Antibacterial, Osteoblast.

### INTRODUCTION

The development of any emerging biomaterial in recent times must satisfy environmental criteria [1]. Therefore, research in the area of biomaterials is focused on the production of biocompatible materials [2]. Naturally derived bioceramic biocomposite materials are also referred to as biocompatible materials and can serve as a viable substitute for the clinical use of current traditional ceramic based biocomposites [3,4]. The substance used for the clinical field must have certain basic features, include biocompatible, non-hazardous, environmental friendly, possessing significant mechanical characteristics and when inserted within the body, must not induce any adverse reactions. There is also an analysis of the mixture of biologically active, highly crystalline, low-cost biocomposite materials required for medical fields [5].

In recent years, different materials, such as hydroxyapatite, bio-ceramics, bioactive glasses, bio-scaffolds, *etc.* were used in biomedical applications [6]. Additionally, owing to its biochemical and crystalline structure resemblance to human bone and teeth tissues, hydroxyapatite has been commonly used for

bone applications. In several biomedical studies, such as bone reconstruction, bone formation and often commonly used as a protective coating for metal implant substrates, hydroxyapatite has been commonly utilized [7]. Although there are numerous chemical techniques to synthesize hydroxyapatite, researchers are still looking for the biologically active hydroxyapatite synthesis process, which is simple, inexpensive, environmentally sustainable and time-saving. Numerous biomimetics strategies are environmentally and close to zero processing and often reduce environmental emissions relative to traditional methods. Few researches have currently been focused on producing hydroxyapatite from animal teeth. It can be clearly shown that the hydroxyapatite naturally-derived is more biocompatible than that acquired from chemical routes. The preparation of animal teeth hydroxyapatite is a practicable, efficient choice that also produces pristine hydroxyapatite [8-10]. The use of biowastes from the meat food processing industry for hydroxyapatite synthesis will significantly mitigate environmental challenges and also offer a strong opportunity to reduce costs in the treatment of bone reconstruction [11].

While hydroxyapatite has outstanding biocompatible characteristics, it is undesirable for load-bearing tissue engineering due to its fragile existence. Polymeric substances are often used to enhance the mechanical efficiency of hydroxyapatite in clinical uses. If used in hydroxyapatite biocomposites, the polymer is bioactive and suitable for clinical field, especially in bone regeneration components [12]. Polymers such as chitosan, gelatin, collagen, polylactic acid, polyacrylic acid and polyvinyl pyrrolidone and owing to their  $\text{Ca}^{2+}$  binding capabilities are generally studied as suitable polymers for the development of biocomposites with hydroxyapatite [13].

Chitosan (CS), which is biologically derived polysaccharide and commonly used as a polymer network for the preparation of hydroxyapatite biocomposites [14]. One of the main biological devices of HA/CS biocomposite is bone insertion, although the mechanical characteristics of hydroxyapatite and chitosan replacements is very poor for bone tissue engineering implementations. Besides, hydroxyapatite is relatively brittle, such that the inclusion of other polymers like polyvinyl pyrrolidone (PVP), poly(ethylene oxide), poly(styrene), carboxymethyl cellulose, gelatin, poly(vinyl alcohol) and so on could affect the mechanical and cytocompatibility of various tissue engineering applications [15-17]. Of these polymers, polyvinyl pyrrolidone was selected since, it is a water-soluble synthetic biocompatible material and used in the several clinical fields [18]. The inclusion of polyvinyl pyrrolidone in the composite would improve bioavailability with human tissue. A variety of experiments have rarely been described in the mixture of PVP-CS and HA-PVP for future medical applications and are simple to obtain a uniform combination with each other [19].

Another significant problem is that in these therapeutic applications, the biocomposite component becomes a loss due to contamination triggered by microbial interactions or the human body's reaction to the biocomposite when inserted within the body [20]. Ultimately, this incident resulted in hindering cell growth. It is also beneficial to produce a biocomposite material with an outstanding antibacterials nature to cope with contamination or infection at the time of surgery. Several researches on the use of aloe vera in conjunction with biocomposite for improved antibacterial effects [21]. Amino acids found in aloe vera are stated to have a key role to play in the growth and repair of hard tissue [22]. Aloe vera, combined with ceramic content, has become increasingly interested in medical fields as it can be conveniently customized and transported based on specifications [23,24].

The present study aims to produce a mechanically strong, antibacterial and good biocompatibility material for its outstanding use in the medical field in particular in the production of an effective biocompatible implant-bone biomaterial. Hence, the development of hydroxyapatite-derived biowaste strengthened with CS-PVP and aloe vera for various biomedical applications is undertaken. No report on the unique biocomposite has been undertaken to investigate the feasibility of exhibiting improved mechanical, antimicrobial and good biocompatibility. For its mechanical and *in vitro* antimicrobial activities, the prepared biocomposite was evaluated. The prepared biocomposite has interesting applications in different clinical

field owing to its high mechanical properties and outstanding cytocompatibility.

## EXPERIMENTAL

**Preparation of hydroxyapatite from biowaste:** The buffalo teeth had been selected as the raw resources for this research. Buffalo teeth was directly obtained from the nearest meat market. They were first washed with bistouries and boiled in a pot at 100 °C for 6 h. After, the buffalo teeth were carefully transformed into a powder in a porcelain mortar. The material was then heated at 900 °C for 4 h in order to produce a white BT-HA substance.

**Preparation of (BT-HA/CS-PVP) biocomposite:** The research process was used to prepare the BT-HA/CS-PVP biocomposite sample. Briefly, BT-HA material (40 wt.%) was applied to the chitosan (1 wt.%) solution. Afterwards the PVP (1 wt.%) was formulated using double distilled water and applied to all of the above combination, then the solution was poured at room temperature for 24 h through mechanical stirring to form an uniform solution, then the mixture was moved to glass petri plates and dried a BT-HA/CS-PVP biocomposite at room temperature.

**Preparation of (CS-HAP/PVP/ALV) biocomposite:** The reached maturity healthy aloe vera leaves had been harvested from the farmers market, Tamilnadu state, India. Entire aloe vera leaves were cleaned with double distilled water to remove the debris from the substrate. The skin was gently removed from the parenchyma by a knife. The fillets were cleaned vigorously with purified water to extract the vasculature from their structures. The fillets were homogenized in the processor and the heterogeneous mass was purified. Then the precipitate gel was extracted, lyophilized and deposited below -10 °C for the processing of aloe vera powder. The aloe vera material (1 wt.%) was coated with the biocomposite of BT-HA/CS-PVP. In order to obtain optimum distribution, the pH of the composite formulations was kept at 10 and was magnetically stirred for 6 h. The suspension was maintained for 1 day for ageing and then extracted and dried for 24 h in a hot air oven at 50 °C and then processed into a powder form.

**Physico-chemical characterization:** Fourier transform infrared spectroscopy (FTIR Spectrometer, Bruker) were collected in the range 4000-500  $\text{cm}^{-1}$ . XRD analysis of prepared samples was carried out by Rigaku Mini Flex 660 with an X-ray source of  $\text{CuK}\alpha$  radiation over the range of 2 $\theta$  angle 10-80°. The morphology and elemental composition of the prepared samples were examined by using FESEM (Carl Zeiss) equipped with EDX. The hardness tests of the prepared specimen were carried out using the Vickers microhardness test method (Shimadzu), 200 g load for 20 s.).

**Biological characterization:** The prepared samples were tested for its antimicrobial behaviour using the agar disc diffusion system against two bacterial strains *S. aureus* and *E. coli*. The Whatman filter paper was used to create discs of size 4 mm and instead soaked in prepared samples, put at equivalent intervals and then hatched at 37 °C. The zone of inhibition all over the disc of the prepared samples was determined for the estimation of antimicrobial property against the two strains of bacteria.

Hemocompatibility was calculated by the use of the haemolytic analysis as reported [25]. For the assay procedure, the osteoblast cells were seeded at a density of  $1 \times 10^4$  cells over the prepared sample in 96 culture plate to assess cell proliferation in 1, 3 and 7 days of incubation period. The prepared samples were collected from the well plates after the incubation time and then cleaned with the PBS solution. With a UV-spectrophotometer, the absorbance was estimated at 570 nm.

## RESULTS AND DISCUSSION

**FTIR studies:** FTIR spectroscopy was used to categories the presence of functional groups in BT-HA/CS-PVP/ALV biocomposites as seen in Fig. 1a. The FTIR spectrum for BT-HA is seen in Fig. 1a, showing the bands at  $608 \text{ cm}^{-1}$  and  $555 \text{ cm}^{-1}$  referring to the bending mode for phosphate groups, while the bands referring to the stretching modes for phosphate groups occur at  $1096$ ,  $1029$  and  $935 \text{ cm}^{-1}$ , respectively [26]. It may be well known that bands referring to hydroxyapatite, which promote the development of hydroxyapatite-derived buffalo teeth (biowaste) were identified [27]. The FTIR spectrum of BT-HA/CS-PVP displays the characteristic peaks to BT-HA along with the bands of CS-PVP to support the development of BT-HA/CS-PVP biocomposite (Fig. 1b). In addition, the wide and strong absorption spectrum at  $3394$  is attributable to the symmetrical stretching vibration of  $\text{OH}^-$  in chitosan and the signature band at  $2901 \text{ cm}^{-1}$  reflects the  $\text{CH}_2$  asymmetric stretching vibration in PVP [28]. The peak at  $1642 \text{ cm}^{-1}$  is related to  $\text{C}=\text{O}$  bending vibration of PVP. At  $2901 \text{ cm}^{-1}$  and  $1256 \text{ cm}^{-1}$ , respectively, the C-H and C-N peaks contribute to the stretching vibration of composite PVP with BT-HA/CS-PVP (Fig. 1b). There is a functional group referring to BT-HAP, BT-HAP/CS-PVP and together with it, bands promoting aloe vera activity in BT-HAP/CS-PVP biocomposite that support BT-HAP/CS-PVP/ALV biocomposite forming was also identified (Fig. 1c). The functional group of constituents defined as glucan units contained in aloe vera demonstrated their related peak at  $1428 \text{ cm}^{-1}$ . In comparison, the most significant aloe vera pyranoside ring and mannose absorption band were observed at  $1043 \text{ cm}^{-1}$ , indicating the existence of aloe vera in the composite BT-HAP/CS-PVP/ALV [29]. Therefore, the FTIR spectrim in Fig. 1c display all the typical bands for BT-HA, CS-PVP and aloe vera that help the development of the BT-HAP/CS-PVP/ALV bio-composite.

**XRD studies:** Fig. 2 displays the obtained XRD pattern of BT-HA, BT-HP/CS-PVP and BT-HP/CS-PVP/AVL biocomposites. The XRD patterns of biocomposite showed that the diffraction trends and intensities relate to the hydroxyapatite phase with JCPD card no. 09-0432 [30]. The BT-HA/CS-PVP biocomposite XRD patterns exhibit the planes corresponding to hydroxyapatite with the peaks corresponding to (402), (213), (310), (202), (300), (211) and (002), authenticates the development of phase pristine hydroxyapatite [31]. Beside with this, the planes corresponding to chitosan and PVP show at  $\sim 16^\circ$  and  $22^\circ$  [28]. The XRD patterns of BT-HA/CS-PVP/AVL biocomposite that confirm the existence of peaks corresponding to hydroxyapatite. The estimated  $2\theta$  values in the spectrum

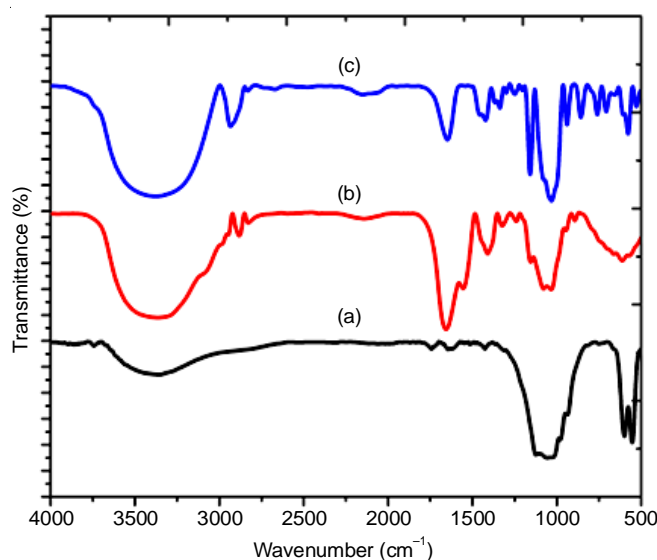


Fig. 1. FTIR pattern of (a) BT-HA, (b) BT-HA/CS-PVP and (c) BT-HA/CS-PVP/ALV biocomposite

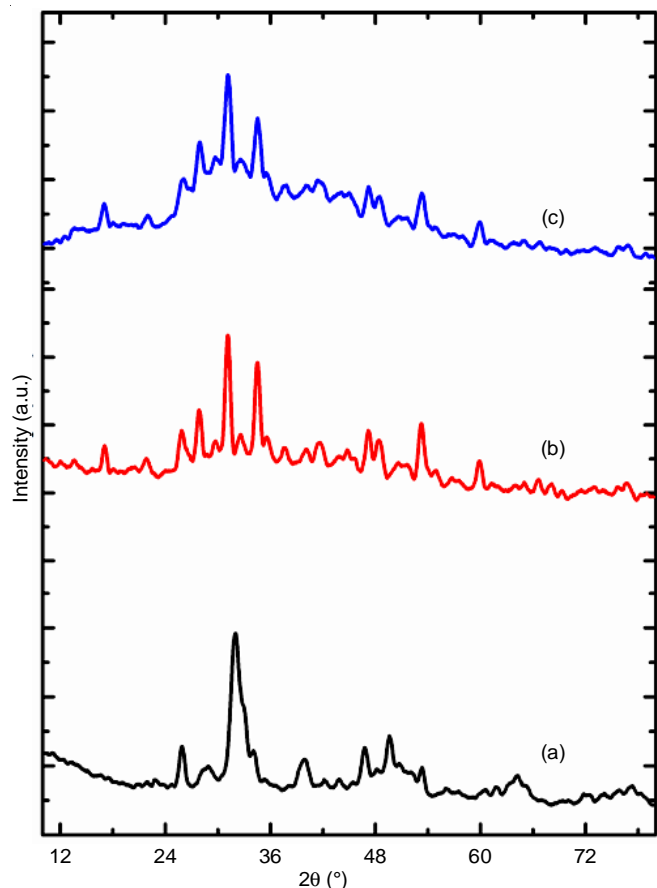


Fig. 2. XRD pattern of (a) BT-HA, (b) BT-HA/CS-PVP and (c) BT-HA/CS-PVP/ALV biocomposite

show the representation of 202 and 002 planes, suggesting the existence of hydroxyapatite, while the CS-PVP peaks that tend to be  $16^\circ$  and  $22^\circ$  did not alter. In contrast, there are peaks referring to aloe vera with  $2\theta$  peaks of  $11^\circ$ ,  $20^\circ$  and  $24^\circ$  referred to (110) (110) and (336), respectively [32]. Therefore, the prepared BT-HA/CS-PVP/AVL biocomposite displays only the

signature plans of hydroxyapatite, indicating that its phase did not shift with the addition of CS-PVP and aloe vera. A major expansion of these diffraction peaks was observed, signaling a decline in the presence of CS-PVP in hydroxyapatite crystallinity. A interested in extending of such diffraction peaks has been reported, suggesting a decrease in the presence of CS-PVP in hydroxyapatite crystallinity [33].

**Morphological studies:** The SEM study was used to analyze the surface characteristics of BT-HA and its biocomposite with CS-PVP and aloe vera. The development of well-dispersed, almost flaks particles discrete BT-HA particles is seen in Fig. 3a. The whole specimen is almost dispersed by these identical discrete particles. On inclusion of CS-PVP to BT-HA/CS-PVP biocomposite Fig. 3b, several interconnected pores were found between mixture components. The CS-HAP/PVP biocomposite morphology indicates that the pore structure can cause material to flow through or encourage cells and tissues to bind to one another [34]. Fig. 4 displays the SEM morphology of BT-HA/CS-PVP/ALV. Contrasted to BT-HAP, BT-HA/CS-PVP biocomposite, the morphology acquired for BT-HA/CS-PVP/ALV biocomposite is quite distinguishable. Therefore when the addition of aloe vera to the biocomposite, irregular clusters began to vanish, the biocomposite pattern produced a matrix (Fig. 3c). It is also clear that HA/CS-PVP/ALV biocomposite can be useful for the flow of physiological fluid that facilitates cell proliferation that is most suitable for clinical use. Fig. 3d displays the EDX spectrum in biocomposites. The EDX results showed that Ca, P, O and C respectively, are the elements found in the biocomposite.

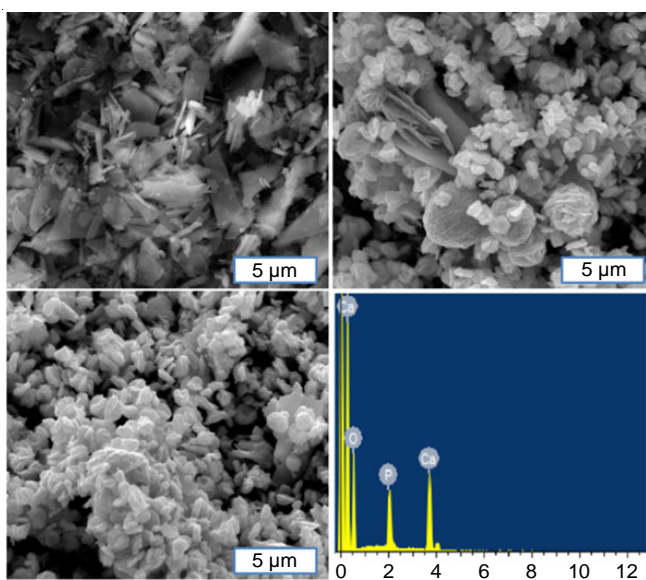


Fig. 3. SEM image of (a) BT-HA, (b) BT-HA/CS-PVP, (c) BT-HA/CS-PVP/ALV and (d) EDAX spectrum of BT-HA/CS-PVP/ALV biocomposite

**Mechanical studies:** Sufficient mechanical characteristics must be correlated with the hydroxyapatite based biocomposite to be used for different clinical field [35]. The primary concern for the development of hydroxyapatite/polymer biocomposites is to enhance the mechanical properties of hydroxyapatite materials for their clinical field, particularly in the orthopedic

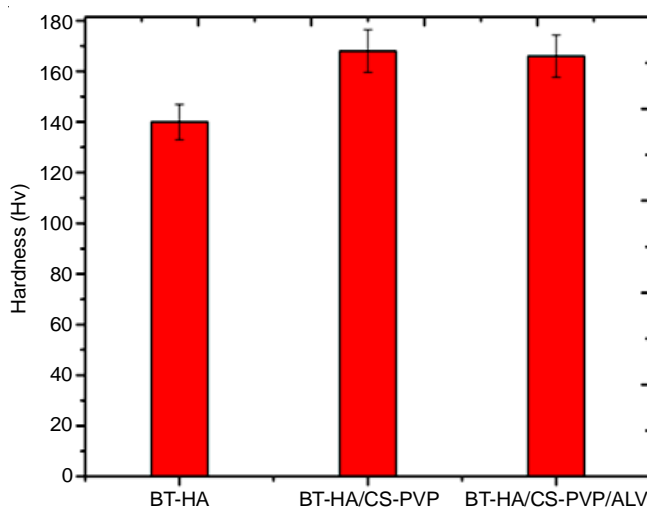


Fig. 4. Micro hardness of prepared samples

field. The mechanical characteristics of the prepared biocomposite were examined in this analysis and the descriptions are presented in Fig. 5. It is obvious that as the incorporation of CS-PVP to BT-HAP/CS-PVP biocomposite raises the hardness values. Due to the strong dispersion of BT-HA in CS-PVP, the rise in the hardness value of CS-PVP in BT-HA can possibly contribute. Furthermore, the introduction of aloe vera to the biocomposite of BT-HAP/CS-PVP/ALV did not change the mechanical characteristics of the biocomposite material prepared.

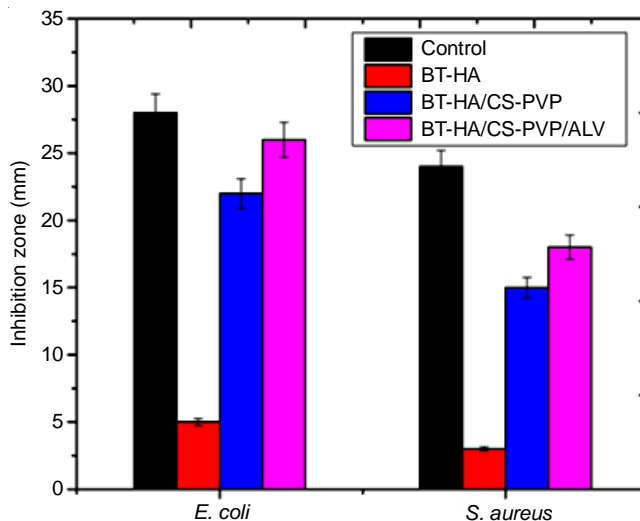


Fig. 5. Antibacterial activity of prepared samples against *E. coli* and *S. aureus* bacteria

**Antibacterial activity:** The substance to be used for the medicinal utilization in the field of inflammation and infection dissolution compromising its cytocompatibility, have inhibitory effects against pathogenic bacteria [36]. Therefore, the antimicrobial action of CS-HAP, CS-HAP/PVP and CS-HAP/PVP/AV composites prepared at against Gram-positive and Gram-negative microbes was assessed and contrasted with control. The average was measured for three replications of the inhibition zone around each disc for various substance concentrations. The results showed that BT-HA/CS-PVP/ALV

demonstrated a good antimicrobial activity among the various materials. This is largely because of the inclusion of aloe vera in the biocomposite. In comparison, action against *E. coli* is observed to be higher than *S. aureus*, likely due to the disparity between the Gram-negative and the Gram-positive microbiota in the cell membrane. Integrating all these considerations, it is obvious that the CS-HAP/PVP/AV composite has favourable antimicrobial properties that are important for clinical field.

**Hemocompatibility assay:** In attempt to comprehend the consistency of prepared biomaterials with blood samples and the associations among them, haemolysis analysis is one of the most significant cytotoxicity studies [37]. The association between biomaterials and blood produces multiple *in vivo* reactions. To prevent adverse interactions between newly prepared materials and blood, it is therefore important to research blood compatibility. The hemocompatibility test findings are displayed in Fig. 6. The hemolytic level was smaller than 2 percent, suggesting that all biocomposites were extremely hemocompatible. BT-HA/CS-PVP/ALV reveals the very least hemolytic percentage (less than 2%) among all composites and biocomposite is much more strongly hemocompatible due to presence of aloe vera. The current research indicates the very least hemolytic proportion according to the literature, so this biocomposite is ideal for orthopedic implant uses.

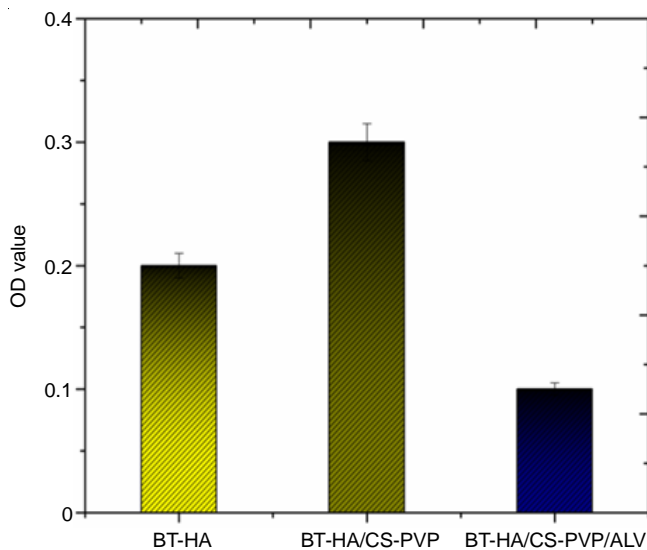


Fig. 6. *In vitro* hemolytic activity of prepared samples

***In vitro* bioactivity study:** The SEM representation of biocomposite after immersion at various time periods in the SBF solution is shown in Fig. 7, which indicates that the more hydroxyapatite layer on the biocomposite surface is placed as period rises. Because of the existence of BT-HA, the nucleation and hydroxyapatite layer formation was started at the start itself. The calcium phosphate existing in the SBF solution achieved passivation in the solution with an increase in contact time, which improved accumulation and the fresh bone-like apatite coating on the biocomposite material surface [38].

***In vitro* cell viability:** The MTT assay test was used for this objective to assess the cytocompatibility of the prepared biocomposites using osteoblast cells. The biocomposites were

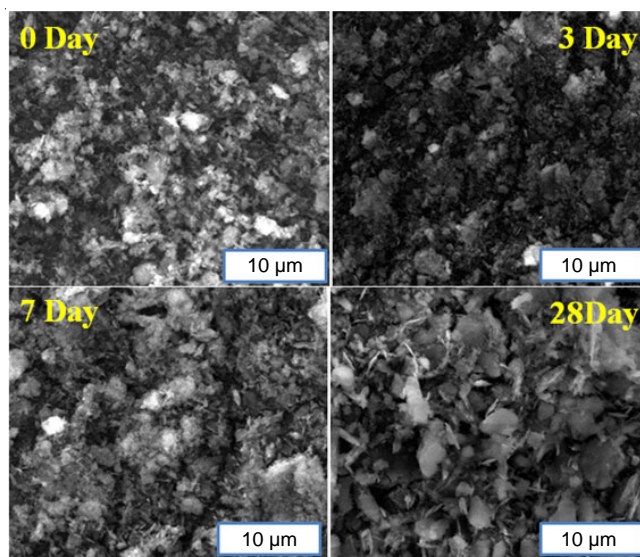


Fig. 7. SEM images of BT-HA/CS-PVP/ALV biocomposite; before and after immersion in SBF for different days

incubated with osteoblast cells and the optical densities for cell growth in the biocomposites were calculated after 1, 3, 7 days of incubation. A significant absorbance reading of 90 percent viable cells is recorded for BT-HA/CS-PVP/ALV from day 7 of culturing as biocomposite are contrasted to other specimens (Fig. 8). It may be attributed to the existence of BT-HA and aloe vera contributing to beneficial cell growth and increased biocompatibility.

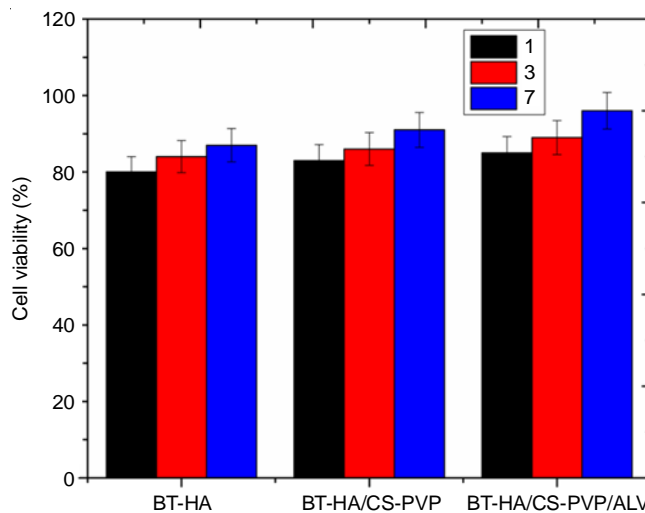


Fig. 8. Bar diagram showing the percentage cell viability of prepared samples against osteoblast cell

In addition, the osteoblast cells can be most effectively connected, growth and differentiate on hydroxyapatite-based biocomposites. Fig. 9 displays the fluorescence microscopic images of prepared samples. Cell viability was observed to be maximum for hydroxyapatite. It is noticed that cell viability is maximal for BT-HA/CS-PVP/ALV. Since, hydroxyapatite is the main component of real bones and teeth and has strong cytocompatibility, it helps to improve biocomposite cytocompatibility. Additionally, the existence of aloe vera plays

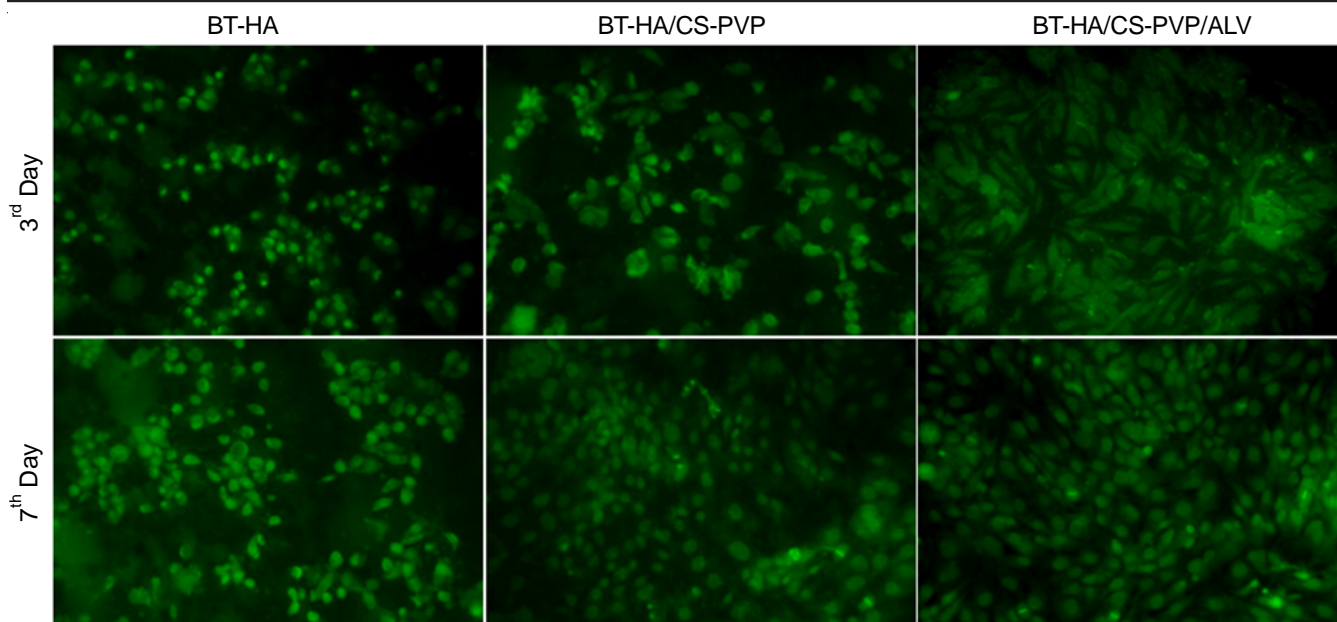


Fig. 9. Fluorescence microscopic images of prepared samples for 3 and 7 days of incubation

an essential role in the biocomposite's enhanced cytocompatible characteristics [39].

### Conclusion

Therefore in the present investigation, the biowaste derived buffalo teeth-derived hydroxyapatite (BT-HA) was constructed of biocomposites with diverse concentrations of chitosan-polyvinyl pyrrolidone (CS-PVP) and aloe vera. The morphology acquired for the biocomposite demonstrated a suitable structure for cell growth, which increases the cytocompatibility of the biocomposite. The involvement of CS-PVP in the biocomposite material plays a major role in improving the mechanical properties of the biocomposite material. In general, the improvement in the viable cells shows that the prepared biocomposite could be more successful in the prevention of bone fractures. In view of improved mechanical properties and high antibacterial, hemocompatibility, cytocompatibility, the prepared BT-HA/CS-PVP/ALV biocomposite would have interesting applications in different regenerative medicine.

### CONFLICT OF INTEREST

The authors declare that there is no conflict of interests regarding the publication of this article.

### REFERENCES

1. K. Manivannan, G. Jaganathan, M. A. Sithique, *J. Sci.: Adv. Mater. Devices*, **6**, 197 (2021); <https://doi.org/10.1016/j.jsamd.2021.01.001>
2. G. Priya, N. Vijayakumari and R. Sangeetha, *J. Sci.: Adv. Mater. Devices*, **3**, 317 (2018); <https://doi.org/10.1016/j.jsamd.2018.06.002>
3. M. Bongio, J.J. Van Den Beucken, S.C. Leeuwenburgh and J.A. Jansen, *J. Mater. Chem.*, **20**, 8747 (2010); <https://doi.org/10.1039/c0jm00795a>
4. F. Sun, H. Zhou and J. Lee, *Acta Biomater.*, **7**, 3813 (2011); <https://doi.org/10.1016/j.actbio.2011.07.002>
5. A. Esmailkhanian, F. Sharifianjazi, A. Abouchenari, A. Rouhani, N. Parvin and M. Irani, *Appl. Biochem. Biotechnol.*, **189**, 919 (2019); <https://doi.org/10.1007/s12010-019-03046-6>
6. O. Kirdök, T.D. Altun, D. Dokgöz and A. Tokuç, *Int. J. Glob. Warm.*, **19**, 127 (2019); <https://doi.org/10.1504/IJGW.2019.101776>
7. Y. Chen, W. Li, C. Zhang, Z. Wu and J. Liu, *Adv. Healthcare Mater.*, **9**, 2000724 (2020); <https://doi.org/10.1002/adhm.202000724>
8. A. Elkayar, Y. Elshazly and M. Assaad, *Bone Tissue Regen. Insights*, **2**, BTRI.3728 (2009); <https://doi.org/10.4137/BTRI.S3728>
9. N. Akyurt, M. Yetmez, U. Karacayli, O. Gunduz, S. Agathopoulos, H. Gökçe, M. Öveçoglu and F. Oktar, *Key Eng. Mater.*, **493-494**, 281 (2012); <https://doi.org/10.4028/www.scientific.net/KEM.493-494.281>
10. S. Salman, O. Gunduz, S. Yilmaz, M.L. Ovecoglu, R.L. Snyder, S. Agathopoulos and F.N. Oktar, *Ceram. Int.*, **35**, 2965 (2009); <https://doi.org/10.1016/j.ceramint.2009.04.004>
11. S.L. Bee and Z.A. Hamid, *Ceram. Int.*, **46**, 17149 (2020); <https://doi.org/10.1016/j.ceramint.2020.04.103>
12. G. Kaur, V. Kumar, F. Baimo, J.C. Mauro, G. Pickrell, I. Evans and O. Bretcanu, *Mater. Sci. Eng. C*, **104**, 109895 (2019); <https://doi.org/10.1016/j.msec.2019.109895>
13. M. Abbasian, B. Massoumi, R. Mohammad-Rezaei, H. Samadian and M. Jaymand, *Int. J. Biol. Macromol.*, **134**, 673 (2019); <https://doi.org/10.1016/j.ijbiomac.2019.04.197>
14. J. Huang, J. Ratnayake, N. Ramesh and G.J. Dias, *ACS Omega*, **5**, 16537 (2020); <https://doi.org/10.1021/acsomega.0c01168>
15. S.S. Garakani, S.M. Davachi, Z. Bagher, A.H. Esfahani, N. Jenabi, Z. Atoufi, M. Khanmohammadi, A. Abbaspourrad, H. Rashedi and M. Jalessi, *Int. J. Biol. Macromol.*, **164**, 356 (2020); <https://doi.org/10.1016/j.ijbiomac.2020.07.138>
16. V. Narayanan, S. Sumathi and A.N.R. Narayanasamy, *J. Biomed. Mater. Res. A*, **108**, 1867 (2020); <https://doi.org/10.1002/jbm.a.36950>
17. K.S. Ogueri, T. Jafari, J.L. Escobar Ivirico and C.T. Laurencin, *Regen. Eng. Transl. Med.*, **5**, 128 (2019); <https://doi.org/10.1007/s40883-018-0072-0>
18. M. Kurakula and G.K. Rao, *J. Drug Deliv. Sci. Technol.*, **60**, 102046 (2020); <https://doi.org/10.1016/j.jddst.2020.102046>

19. I.V. Fadeeva, S.M. Barinov and A.S. Fomin, *Inorg. Mater.: Appl. Res.*, **11**, 117 (2020); <https://doi.org/10.1134/S2075113320010116>
20. M. Milazzo, G. Gallone, E. Marcello, M.D. Mariniello, L. Bruschini, I. Roy and S. Danti, *J. Funct. Biomater.*, **11**, 60 (2020); <https://doi.org/10.3390/jfb11030060>
21. M. Nikbakht, M. Salehi, S.M. Rezaya and R.F. Majidi, *Nanomed. J.*, **7**, 21 (2020); <https://doi.org/10.22038/nmj>
22. S. Samadieh and M. Sadri, *Nanomedicine Res. J.*, **5**, 1 (2020); <https://doi.org/10.22034/NMRJ.2020.01.001>
23. D. Banerjee and S. Bose, *ACS Appl. Bio Mater.*, **2**, 3194 (2019); <https://doi.org/10.1021/acsabm.9b00077>
24. S. Shanmugavel, V.J. Reddy, S. Ramakrishna, B.S. Lakshmi and V.G. Dev, *J. Biomater. Appl.*, **29**, 46 (2014); <https://doi.org/10.1177/0885328213513934>
25. G. Radha, S. Balakumar, B. Venkatesan and E. Vellaichamy, *Mater. Sci. Eng. C*, **50**, 143 (2015); <https://doi.org/10.1016/j.msec.2015.01.054>
26. R. Ranjan, A.M. Kayastha and N. Sinha, *Biophys. Chem.*, **265**, 106430 (2020); <https://doi.org/10.1016/j.bpc.2020.106430>
27. A.M. Patil, V.V. Gite, H.D. Jirimali and R.N. Jagtap, *J. Polym. Environ.*, **29**, 799 (2020); <https://doi.org/10.1007/s10924-020-01903-8>
28. Q. Yao, W. Li, S. Yu, L. Ma, D. Jin, A.R. Boccaccini and Y. Liu, *Mater. Sci. Eng. C*, **56**, 473 (2015); <https://doi.org/10.1016/j.msec.2015.06.046>
29. H. Wang, X. Zhang, M.P. Mani, S.K. Jaganathan, Y. Huang and C. Wang, *Coatings*, **7**, 182 (2017); <https://doi.org/10.3390/coatings7110182>
30. D. Predoi, S.L. Iconaru and M.V. Predoi, *Coatings*, **10**, 905 (2020); <https://doi.org/10.3390/coatings10090905>
31. R. Prahraj, S. Mishra, R.D.K. Misra and T.R. Rautray, *Mater. Technol.*, **37**, 230 (2022); <https://doi.org/10.1080/10667857.2020.1825898>
32. S.M.L. Gontijo, A.D.M. Gomes, A. Gala-García, R.D. Sinisterra and M.D. Cortés, *Elec. J. Biotechnol.*, **16**, 1 (2013).
33. Y. Guesmi, H. Agougui, M. Jabli and A.M. Alsharabasy, *Chem. Eng. Commun.*, **206**, 279 (2019); <https://doi.org/10.1080/00986445.2018.1486302>
34. X. Li, H.M. Yin, K. Su, G.S. Zheng, C.Y. Mao, W. Liu, P. Wang, Z. Zhang, J.Z. Xu, Z.M. Li and G.Q. Liao, *ACS Biomater. Sci. Eng.*, **5**, 2998 (2019); <https://doi.org/10.1021/acsbiomaterials.9b00209>
35. V. Chopra, J. Thomas, A. Sharma, V. Panwar, S. Kaushik and D. Ghosh, *Mater. Sci. Eng. C*, **119**, 111584 (2021); <https://doi.org/10.1016/j.msec.2020.111584>
36. W. Weng, X. Li, W. Nie, H. Liu, S. Liu, J. Huang, Q. Zhou, J. He, J. Su, Z. Dong and D. Wang, *Int. J. Nanomedicine*, **15**, 5027 (2020); <https://doi.org/10.2147/IJN.S241859>
37. M. Bernard, E. Jubeli, J. Bakar, L. Tortolano, J. Saunier and N. Yagoubi, *J. Biomed. Mater. Res. A*, **105**, 3333 (2017); <https://doi.org/10.1002/jbm.a.36199>
38. N.-H. Saddiqi, D. Patra and S. Seeger, *Colloid Interface Sci. Commun.*, **16**, 1 (2017); <https://doi.org/10.1016/j.colcom.2016.12.002>
39. S. Rahman, P. Carter and N. Bhattarai, *J. Funct. Biomater.*, **8**, 6 (2017); <https://doi.org/10.3390/jfb8010006>